

STOCHASTIC FILTERING WITH MOMENT REPRESENTATION *

ZHENG ZHAO[†] AND JUHA SARMAVUORI[‡]

Abstract. Stochastic filtering refers to estimating the probability distribution of the latent stochastic process conditioned on the observed measurements in time. In this paper, we introduce a new class of convergent filters that represent the filtering distributions by their moments. The key enablement is a quadrature method that uses orthonormal polynomials spanned by the moments. We prove that this moment-based filter is asymptotically exact in the order of moments, and show that the filter is also computationally efficient and is in line with the state of the art.

Key words. Stochastic filtering, state space, moment, characteristic function, Gaussian quadrature, Kalman filter, stochastic differential equation

MSC codes. 60G35, 62M05, 62M20, 65D32, 65C60

1. Introduction. In this manuscript, we study the filtering problem concerned with models of the form

$$(1) \quad \begin{aligned} dX(t) &= a(X(t)) dt + b(X(t)) dW(t), \\ X_0 &\sim \mathbb{P}_{X_0}, \\ Y_k | X_k &\sim p_{Y_k | X_k}, \end{aligned}$$

where the process $\{X(t) \in \mathbb{R}^d : t \geq 0\}$ solves the Itô stochastic differential equation (SDE) defined by a standard Wiener process $\{W(t) \in \mathbb{R}^{d_w} : t \geq 0\}$, drift function $a: \mathbb{R}^d \rightarrow \mathbb{R}^d$, dispersion function $b: \mathbb{R}^d \rightarrow \mathbb{R}^{d \times d_w}$, and initial distribution \mathbb{P}_{X_0} . The random variable $Y_k \in \mathbb{R}^{d_y}$ stands for the measurement of $X_k := X(t_k)$ at any discrete time t_k following a given conditional probability density function (PDF) $p_{Y_k | X_k}$. In addition, if X is a discrete-time process instead of a solution to the SDE above, we only require that the conditional expectation $\mathbb{E}[g(X_k) | X_{k-1}]$ is computable for any polynomial g .

The filtering problem refers to solving the probability distribution $\mathbb{P}_{X_k | Y_{1:k}}$ of X_k conditioned on the collection of measurements $Y_{1:k} := \{Y_1, Y_2, \dots, Y_k\}$ for $k = 1, 2, \dots$. This is a classical problem, and it is known to be challenging to compute the exact solution except for some isolated models. In the literature, there are plenty of approximate methods, such as Gaussian filters [17] and particle filters [7], which are arguably the most popular ones. The principle of Gaussian filters (e.g., extended Kalman filters and Gauss–Hermite filters) is to approximate the filtering distribution $\mathbb{P}_{X_k | Y_{1:k}}$ by a Gaussian so that the filtering problem boils down to only computing the mean and covariance of $\mathbb{P}_{X_k | Y_{1:k}}$, which are usually efficient to compute. However, Gaussian approximations do not converge to the actual distribution that is non-Gaussian. In a different flavour, particle filters resort to approximate the filtering distribution by weighted samples, and then make use of sequential Monte Carlo techniques to estimate

*Submitted to the editors DATE.

Funding: This research was partially supported by the Wallenberg AI, Autonomous Systems and Software Program (WASP) funded by Knut and Alice Wallenberg Foundation. The computations handling was enabled by resources provided by the National Academic Infrastructure for Supercomputing in Sweden (NAISS) and the Swedish National Infrastructure for Computing (SNIC) partially funded by the Swedish Research Council through grant agreements no. 2022-06725 and no. 2018-05973.

[†]Department of Information Technology, Uppsala University, Sweden (zheng.zhao@it.uu.se).

[‡]Department of Electrical Engineering and Automation, Aalto University, Finland (juha.sarmavuori@aalto.fi).

these weights and samples recursively in time. Under mild system conditions, the particle filters are convergent in the number of samples [1, 7]. However, to converge fast, we need a large number of samples, which in turn make the filtering routine computationally demanding and memory-consuming. It is also a common problem that sequential Monte Carlo methods can produce degenerate or impoverished weights, and solving such problems often incurs additional computations.

There are also convergent filters by approximating the solution to the Kushner–Stratonovich equation. Examples are projection filters [3, 12] which project the filtering densities onto finite-dimensional manifolds. However, these filters are primarily concerned with continuous-time measurements, while we focus on the discrete-time setting. Hence, we do not relate them to the scope of this paper. For detailed reviews of stochastic filters and their properties, we refer the readers to, for instance, [18, 1, 29, 25].

1.1. Contributions. We introduce a new class of asymptotically exact and efficient filters to solve the filtering problem in Equation (1). Specifically, we represent the filtering distribution $\mathbb{P}_{X_k | Y_{1:k}}$ by a sequence of its moments, and then we recursively estimate this sequence for $k = 1, 2, \dots$ by using a moment-based quadrature method. To expose the idea, let us suppose that X is unidimensional (i.e., $d = 1$). Then, at each time t_k , we use a sequence of $2N$ moments

$$(2) \quad \begin{aligned} M_k^N &:= \{m_{k,0}, m_{k,1}, m_{k,2}, \dots, m_{k,2N-1}\}, \\ m_{k,n} &:= \mathbb{E}[X_k^n | Y_{1:k}] := \int x^n d\mathbb{P}_{X_k | Y_{1:k}}(x), \end{aligned}$$

to approximately represent $\mathbb{P}_{X_k | Y_{1:k}}$. Note that $m_{k,0} = 1$ by definition. This moment-based representation converges in distribution as $N \rightarrow \infty$, if the target distribution $\mathbb{P}_{X_k | Y_{1:k}}$ is determined by its moments (see, e.g., [21, Chap. 15] for sufficient conditions). Now suppose that we explicitly know the moments M_0^N of the initial $\mathbb{P}_{X_0 | Y_{1:0}} := \mathbb{P}_{X_0}$. We show a quadrature method so that we can use M_0^N to approximate the moments M_1^N of the next filtering distribution $\mathbb{P}_{X_1 | Y_{1:1}}$, denoted by \widehat{M}_1^N . Likewise, we then continue to compute \widehat{M}_k^N based on \widehat{M}_{k-1}^N , and so forth for $k = 2, 3, \dots$. This quadrature method generates the quadrature rules based on the orthonormal polynomials spanned by the moments, which is in a similar spirit as the Golub–Welsch approach [16].

Our proposed moment filter is a significant contribution to the community in terms of convergence and computation. We prove that at any time t_k , the approximate moments \widehat{M}_k^N converge to the true moments as $N \rightarrow \infty$ under mild conditions of the system. Moreover, if the true filtering distributions are determined by their moments, then the discrete measures generated by the approximate moments and the quadrature method converge weakly to the truth too. In addition, the moment filter simultaneously gives a consistent and differentiable likelihood approximation which we can use to estimate the model parameters by maximum likelihood. The experiments show that the moment filter converges numerically as $N \rightarrow \infty$, and that the convergence speed is substantially faster than that of standard particle filters. While controlling the particle filter to have a similar computation time as the moment filter, the moment filter is significantly more accurate than the particle filter by a few orders of magnitude.

1.2. Structure. The paper is structured as follows. In Section 2, we present the unidimensional quadrature method based on moments, and then we generalise the

method for multidimensional systems. In Section 3, we derive the filter with moment representations, and then we show how to apply the introduced moment quadrature method to the moment filter. In the same section, we prove that the moment filter converges in distribution and moments. The numerical results are shown in Section 4, followed by conclusions and discussions in Section 5. Finally, in Section 6, we discuss the related works for comparison to our method.

2. Quadrature with moments. Let $X \in \mathbb{R}^d$ be a random variable and \mathbb{P} be its probability distribution/measure. For clarity, we for now assume that the dimension $d = 1$. The essence of the filtering problem that we aim to solve consists in computing the integral

$$\mathbb{E}[f(X)] := \int f(x) d\mathbb{P}(x) \approx \sum_{n=1}^N w_n f(\lambda_n),$$

by a set of quadrature rules $\{w_n, \lambda_n\}_{n=1}^N$, and the quadrature rules are to be determined by the moments $m_n := \mathbb{E}[X^n]$ of the measure \mathbb{P} . A straightforward solution is to approximate the integrand f by a power series. Then the integral is approximated by a sum of moments weighted by the derivatives of f . However, this approach has limited applications, as it requires the integrand to be analytic which is a restrictive condition. Moreover, computing high-order derivatives is computationally demanding.

To solve this moment-quadrature problem, we formulate a system of orthonormal polynomials, the coefficients of which are defined by the moments, and then we use the roots of the polynomial with the highest degree as the quadrature nodes [16, 15]. By using this approach, the quadrature approximation is exact for any polynomial f of degrees equal to or less than $2N - 1$ with moments $M^N := \{m_n\}_{n=0}^{2N-1}$. This in turn means that the quadrature is asymptotically exact in N for any continuous f on a compact domain by Weierstrass theorem. We detail this approach in the following.

Let us define an inner product $\langle f, g \rangle := \int f g d\mathbb{P} = \mathbb{E}[f(X)g(X)]$, and denote ψ_n an orthonormal polynomial of degree n . It is well-known that any orthonormal polynomial system $\psi = \{\psi_0, \psi_1, \dots, \psi_N\}$ in terms of this inner product is uniquely characterised by a three-term recurrence relation [14, 15]

$$(3) \quad \beta_{n+1} \psi_{n+1}(x) = (x - \alpha_{n+1}) \psi_n(x) - \beta_n \psi_{n-1}(x), \quad n = 0, 1, \dots, N - 1,$$

where

$$\begin{aligned} \psi_{-1}(x) &:= 0, \quad \psi_0(x) = 1, \quad \text{for all } x, \\ \alpha_n &= \langle \psi_{n-1}, Z\psi_{n-1} \rangle, \quad n = 1, 2, \dots, N, \\ \beta_0 &= 1, \quad \beta_n = \langle \psi_n, Z\psi_{n-1} \rangle, \quad n = 1, 2, \dots, N - 1, \end{aligned}$$

and Z is a multiplication operator defined via $(Zg)(x) := xg(x)$ for any function g . If we rewrite the three-term recurrence relation in a vector form [15, pp. 86], the coefficients $\{\alpha_n\}_{n=1}^N$ and $\{\beta_n\}_{n=1}^{N-1}$ constitute a tridiagonal Jacobi matrix

$$(4) \quad J_N := \begin{bmatrix} \alpha_1 & \beta_1 & & & 0 \\ \beta_1 & \alpha_2 & \beta_2 & & \\ & \beta_2 & \ddots & \ddots & \\ & & \ddots & \ddots & \beta_{N-1} \\ 0 & & & \beta_{N-1} & \alpha_N \end{bmatrix}.$$

A classical result by [16] shows that the roots $\{\lambda_n\}_{n=1}^N$ of ψ_N are the eigenvalues of J_N , and that the corresponding quadrature weights $\{w_n\}_{n=1}^N$ are the squares of the first components of the eigenvectors of J_N (i.e., if u_n is the n -th eigenvector of J_N , then $w_n = u_{n,1}^2$, where $u_{n,1}$ is the first component of u_n). Computing the eigendecomposition of J_N is notably efficient, since the Jacobi matrix is tridiagonal.

To find such an orthonormal system whose coefficients $\{\alpha_n\}_{n=1}^N$ and $\{\beta_n\}_{n=1}^{N-1}$ are determined by the moments, we define a system of linearly independent functions $\phi := \{\phi_0, \phi_1, \dots, \phi_{N-1}\}$, where $\phi_n(x) := x^n$. Observing that

$G_N :=$

$$\begin{bmatrix} \langle \phi_0, \phi_0 \rangle & \langle \phi_0, \phi_1 \rangle & \cdots & \langle \phi_0, \phi_{N-1} \rangle \\ \langle \phi_1, \phi_0 \rangle & \langle \phi_1, \phi_1 \rangle & \cdots & \langle \phi_1, \phi_{N-1} \rangle \\ \vdots & \vdots & \ddots & \vdots \\ \langle \phi_{N-1}, \phi_0 \rangle & \langle \phi_{N-1}, \phi_1 \rangle & \cdots & \langle \phi_{N-1}, \phi_{N-1} \rangle \end{bmatrix} = \begin{bmatrix} m_0 & m_1 & \cdots & m_{N-1} \\ m_1 & m_2 & \cdots & m_N \\ \vdots & \vdots & \ddots & \vdots \\ m_{N-1} & m_N & \cdots & m_{2N-2} \end{bmatrix}$$

is a Gram/Hankel matrix of moments, we can then obtain the desired orthonormal system ψ by a Gram–Schmidt orthonormalisation of ϕ . The results in [16] show a straightforward routine to compute the coefficients in Equation (3) by the elements of the Cholesky decomposition of G_N . However, this approach loses two degrees of exactness, since G_N does not contain the terminal moment m_{2N-1} . That is, with $2N$ moments M^N , the method results in a Jacobi matrix of size $N - 1$ which makes the quadrature approximation exact for polynomial integrands of degrees equal to or less than $2N - 3$. To compensate the exactness to up to degree $2N - 1$, we can see the Jacobi coefficients as a matrix representation of the multiplication operator Z in ψ , at the cost of additional computations for solving a linear system [31]. To see this, we define another Hankel matrix of moments

$$\begin{aligned} H_N &:= \begin{bmatrix} \langle \phi_0, Z\phi_0 \rangle & \langle \phi_0, Z\phi_1 \rangle & \cdots & \langle \phi_0, Z\phi_{N-1} \rangle \\ \langle \phi_1, Z\phi_0 \rangle & \langle \phi_1, Z\phi_1 \rangle & \cdots & \langle \phi_1, Z\phi_{N-1} \rangle \\ \vdots & \vdots & \ddots & \vdots \\ \langle \phi_{N-1}, Z\phi_0 \rangle & \langle \phi_{N-1}, Z\phi_1 \rangle & \cdots & \langle \phi_{N-1}, Z\phi_{N-1} \rangle \end{bmatrix} \\ &= \begin{bmatrix} m_1 & m_2 & \cdots & m_N \\ m_2 & m_3 & \cdots & m_{N+1} \\ \vdots & \vdots & \ddots & \vdots \\ m_N & m_{N+1} & \cdots & m_{2N-1} \end{bmatrix} \end{aligned}$$

which is the finite matrix representation of the multiplication operator Z in ϕ . Now let $L_N L_N^\top = G_N$ be the Cholesky decomposition of G_N , we can then transform the matrix representation of the operator Z in ϕ to ψ by

$$(5) \quad L_N^{-1} H_N (L_N^\top)^{-1} = \begin{bmatrix} \langle \psi_0, Z\psi_0 \rangle & \langle \psi_0, Z\psi_1 \rangle & \cdots & \langle \psi_0, Z\psi_{N-1} \rangle \\ \langle \psi_1, Z\psi_0 \rangle & \langle \psi_1, Z\psi_1 \rangle & \cdots & \langle \psi_1, Z\psi_{N-1} \rangle \\ \vdots & \vdots & \ddots & \vdots \\ \langle \psi_{N-1}, Z\psi_0 \rangle & \langle \psi_{N-1}, Z\psi_1 \rangle & \cdots & \langle \psi_{N-1}, Z\psi_{N-1} \rangle \end{bmatrix} \\ = J_N$$

which equals to the Jacobi matrix in Equation (4) by definition.

In summary, with moments M^N , we first use the moments to form the matrices G_N and H_N , and then we take the Cholesky decomposition of G_N and solve the linear

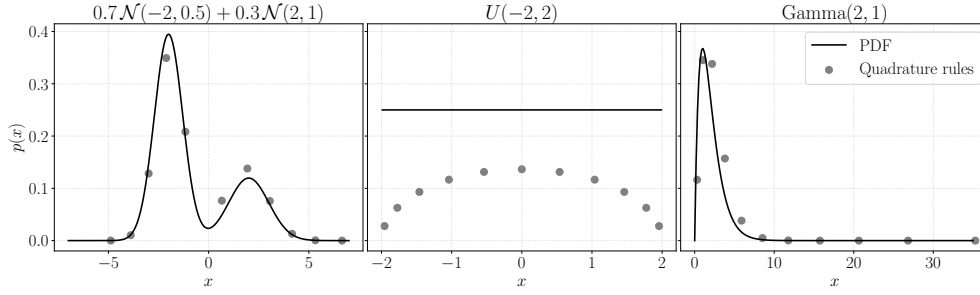


FIGURE 1. Quadrature rules ($N = 11$) for a Gaussian sum (left), a uniform (middle), and a Gamma (right) distribution. The horizontal and vertical locations of the grey points represent the values of the quadrature nodes and weights, respectively. We see that the quadrature rules essentially form a discrete approximation to the continuous distribution, where the discrete probability bins are chosen such that the expectation is exact for up to $2N - 1$ degree polynomials.

system as per Equation (5) to compute J_N . With the Jacobi matrix J_N , we compute its eigenvalues and eigenvectors that we use to determine the quadrature rules. The computational complexity of this quadrature method is dominated by the Cholesky decomposition which is of $O(N^3)$. In Figure 1, we exemplify the quadrature rules generated for three distributions with $N = 11$.

2.1. Generalisation for multidimensional quadrature. Now consider that the dimension $d > 1$. The quadrature method in the previous section no longer applies, since the coefficients of the three-term recurrence relation become vector-valued [10, Chap. 3]. To generalise the quadrature for multidimensional integrations, we resort to view the numerical integration as a finite matrix approximation to a multiplication operator. More specifically, for each dimension, we define a multiplication operator, and then we analogously compute the Jacobi matrix associated for that operator. The resulting quadrature rules are finally given by the Cartesian products of the eigendecompositions of these Jacobi matrices. To detail this generalisation, we introduce the following technical prerequisites.

Let $X_{(i)}$ denote the i -th element of the vector $X \in \mathbb{R}^d$. To define the moments for multidimensional random variables, we introduce multi-index $\mathbf{n} = (n_1, n_2, \dots, n_d)$ of fixed length d , and the exponent $X^{\mathbf{n}}$ reads as the product $X^{\mathbf{n}} := X_{(1)}^{n_1} X_{(2)}^{n_2} \dots X_{(d)}^{n_d}$. As an example, if $d = 3$ and $\mathbf{n} = (5, 1, 4)$, then $X^{\mathbf{n}} = X_{(1)}^5 X_{(2)} X_{(3)}^4$. The collection of moments that we need to generate the quadrature rules is then

$$M^N := \{m_{\mathbf{n}} : |\mathbf{n}| \leq 2N - 1\}, \quad m_{\mathbf{n}} := \mathbb{E}[X^{\mathbf{n}}],$$

where $|\mathbf{n}|$ stands for the sum of the multi-index \mathbf{n} . The collection M^N has in total $\binom{2N-1+d}{2N-1}$ elements, and the elements can be arbitrarily ordered.

Similarly as in Section 2, we define a system of linearly independent basis $\phi := \{\phi_{\mathbf{n}} : |\mathbf{n}| \leq N - 1\}$, where $\phi_{\mathbf{n}}(x) := x^{\mathbf{n}}$, so that they represent the moments. Furthermore, to ensure that our quadrature approximation is valid, we restrict the first basis function in ϕ to be $\phi_{\mathbf{n}_0}(x) = 1$, where the multi-index \mathbf{n}_0 has sum $|\mathbf{n}_0| = 0$. The Gram matrix induced by this system is denoted by G_S with element $(G_S)_{ij} := \langle \phi_{\mathbf{n}_i}, \phi_{\mathbf{n}_j} \rangle$ for $i, j = 0, 1, \dots, S - 1$, where the size of the matrix is $S = \binom{N-1+d}{N-1}$. Since the positive definiteness of the Gram matrix is independent of how we order the basis functions in ϕ , a convenient choice is the graded lexicographical order [10] which has a few nice

properties in favour of indexing and computation.

For each dimension $i = 1, 2, \dots, d$, we introduce a multiplication operator Z_i defined via $(Z_i g)(x) := x_{(i)} g(x)$ for any function $g: \mathbb{R}^d \rightarrow \mathbb{R}$. The finite matrix representation of the operator Z_i in ϕ is defined by

$$H_{S,i} := \begin{bmatrix} \langle \phi_{\mathbf{n}_0}, Z_i \phi_{\mathbf{n}_0} \rangle & \langle \phi_{\mathbf{n}_0}, Z_i \phi_{\mathbf{n}_1} \rangle & \cdots & \langle \phi_{\mathbf{n}_0}, Z_i \phi_{\mathbf{n}_{S-1}} \rangle \\ \langle \phi_{\mathbf{n}_1}, Z_i \phi_{\mathbf{n}_0} \rangle & \langle \phi_{\mathbf{n}_1}, Z_i \phi_{\mathbf{n}_1} \rangle & \cdots & \langle \phi_{\mathbf{n}_1}, Z_i \phi_{\mathbf{n}_{S-1}} \rangle \\ \vdots & \vdots & \ddots & \vdots \\ \langle \phi_{\mathbf{n}_{S-1}}, Z_i \phi_{\mathbf{n}_0} \rangle & \langle \phi_{\mathbf{n}_{S-1}}, Z_i \phi_{\mathbf{n}_1} \rangle & \cdots & \langle \phi_{\mathbf{n}_{S-1}}, Z_i \phi_{\mathbf{n}_{S-1}} \rangle \end{bmatrix}.$$

EXAMPLE 1. Consider $d = 2$ and $N = 2$. Let us choose graded lexicographical ordered multi-indices $\mathbf{n}_0 = (0, 0)$, $\mathbf{n}_1 = (0, 1)$, $\mathbf{n}_2 = (1, 0)$, \dots , $\mathbf{n}_9 = (3, 0)$, so $\phi_{\mathbf{n}_0}(x) = 1$, $\phi_{\mathbf{n}_1}(x) = x_{(2)}$, and $\phi_{\mathbf{n}_2}(x) = x_{(1)}$. Suppose that the ten moments in M^N are ordered by these multi-indices as well. The Gram matrix and the matrices of the two multiplication operators are then

$$G_3 = \begin{bmatrix} 1 & \mathbb{E}[X_{(2)}] & \mathbb{E}[X_{(1)}] \\ \mathbb{E}[X_{(2)}] & \mathbb{E}[X_{(2)}^2] & \mathbb{E}[X_{(1)} X_{(2)}] \\ \mathbb{E}[X_{(1)}] & \mathbb{E}[X_{(1)} X_{(2)}] & \mathbb{E}[X_{(1)}^2] \end{bmatrix} = \begin{bmatrix} m_{\mathbf{n}_0} & m_{\mathbf{n}_1} & m_{\mathbf{n}_2} \\ m_{\mathbf{n}_1} & m_{\mathbf{n}_3} & m_{\mathbf{n}_4} \\ m_{\mathbf{n}_2} & m_{\mathbf{n}_4} & m_{\mathbf{n}_5} \end{bmatrix},$$

$$H_{3,1} = \begin{bmatrix} \mathbb{E}[X_{(1)}] & \mathbb{E}[X_{(1)} X_{(2)}] & \mathbb{E}[X_{(1)}^2] \\ \mathbb{E}[X_{(1)} X_{(2)}] & \mathbb{E}[X_{(1)} X_{(2)}^2] & \mathbb{E}[X_{(1)}^2 X_{(2)}] \\ \mathbb{E}[X_{(1)}^2] & \mathbb{E}[X_{(1)}^2 X_{(2)}] & \mathbb{E}[X_{(1)}^3] \end{bmatrix} = \begin{bmatrix} m_{\mathbf{n}_2} & m_{\mathbf{n}_4} & m_{\mathbf{n}_5} \\ m_{\mathbf{n}_4} & m_{\mathbf{n}_7} & m_{\mathbf{n}_8} \\ m_{\mathbf{n}_5} & m_{\mathbf{n}_8} & m_{\mathbf{n}_9} \end{bmatrix},$$

$$H_{3,2} = \begin{bmatrix} \mathbb{E}[X_{(2)}] & \mathbb{E}[X_{(2)}^2] & \mathbb{E}[X_{(1)} X_{(2)}] \\ \mathbb{E}[X_{(2)}^2] & \mathbb{E}[X_{(2)}^3] & \mathbb{E}[X_{(1)} X_{(2)}^2] \\ \mathbb{E}[X_{(1)} X_{(2)}] & \mathbb{E}[X_{(1)} X_{(2)}^2] & \mathbb{E}[X_{(1)}^2 X_{(2)}] \end{bmatrix} = \begin{bmatrix} m_{\mathbf{n}_1} & m_{\mathbf{n}_3} & m_{\mathbf{n}_4} \\ m_{\mathbf{n}_3} & m_{\mathbf{n}_6} & m_{\mathbf{n}_7} \\ m_{\mathbf{n}_4} & m_{\mathbf{n}_7} & m_{\mathbf{n}_8} \end{bmatrix}.$$

Let $L_S L_S^\top = G_S$ be the Cholesky decomposition of the Gram matrix G_S , then we can compute the matrix representation $\mathring{H}_{S,i}$ of Z_i in an orthonormal basis system $\psi := \{\psi_{\mathbf{n}_0}, \psi_{\mathbf{n}_1}, \dots, \psi_{\mathbf{n}_{S-1}}\}$ by

$$(6) \quad \mathring{H}_{S,i} = L_S^{-1} H_{S,i} (L_S^\top)^{-1},$$

where its u, v -th matrix element $(\mathring{H}_{S,i})_{uv} = \langle \psi_{\mathbf{n}_u}, Z_i \psi_{\mathbf{n}_v} \rangle$, and $\psi_{\mathbf{n}_0}(x) = 1$.

Let $f: \mathbb{R}^d \rightarrow \mathbb{R}$ be any continuous function on a compact domain, and A be any self-adjoint operator. We define the functional operator $f(A)$ as a spectral integral $f(A) := \int_{\sigma(A)} f(z) dP_A(z)$, where P_A is a projection-valued measure induced by A , and $\sigma(A)$ is the spectrum of A . Hence, by $f(Z_1, Z_2, \dots, Z_d)$ we mean that it is an operator $f(Z_1, Z_2, \dots, Z_d) = \int f(z_1, z_2, \dots, z_d) dP_{Z_1}(z_1) dP_{Z_2}(z_2) \cdots dP_{Z_d}(z_d)$. For details of these definitions, see, for instance, [32]. It turns out that $f(Z_1, Z_2, \dots, Z_d)$ is a multiplication operator as well, that is, for any function $g: \mathbb{R}^d \rightarrow \mathbb{R}$,

$$(f(Z_1, Z_2, \dots, Z_d)g)(x) = f(x)g(x).$$

With the property above in mind, we can now think of the quadrature as a finite-matrix approximation to the operator $f(Z_1, Z_2, \dots, Z_d)$. Specifically, the catch is to represent the integral as

$$(7) \quad \int f(x) d\mathbb{P}(x) = \langle \psi_{\mathbf{n}_0}, f \psi_{\mathbf{n}_0} \rangle = \langle \psi_{\mathbf{n}_0}, f(Z_1, Z_2, \dots, Z_d) \psi_{\mathbf{n}_0} \rangle \\ \approx e_0^\top f(\mathring{H}_{S,1}, \mathring{H}_{S,2}, \dots, \mathring{H}_{S,d}) e_0,$$

where $f(\mathring{H}_{S,1}, \mathring{H}_{S,2}, \dots, \mathring{H}_{S,d}) \in \mathbb{R}^{S \times S}$ is a matrix that approximately represents the operator $f(Z_1, Z_2, \dots, Z_d)$, and $e_0 = [1 \ 0 \ \dots \ 0]^\top$ extracts the first component of the matrix. Since we have defined $f(Z_1, Z_2, \dots, Z_d)$ as a spectral integral, the definition of the matrix $f(\mathring{H}_{S,1}, \mathring{H}_{S,2}, \dots, \mathring{H}_{S,d})$ is

$$(8) \quad \begin{aligned} & f(\mathring{H}_{S,1}, \mathring{H}_{S,2}, \dots, \mathring{H}_{S,d}) \\ & := \sum_{n_1=1}^S \sum_{n_2=1}^S \cdots \sum_{n_d=1}^S f(\lambda_{n_1}, \lambda_{n_2}, \dots, \lambda_{n_d}) u_{n_1} u_{n_1}^\top u_{n_2} u_{n_2}^\top \cdots u_{n_d} u_{n_d}^\top, \end{aligned}$$

where λ_{n_i} and u_{n_i} are the n_i -th eigenvalue and eigenvector of the matrix $\mathring{H}_{S,i}$, respectively. Now by substituting Equation (8) back into Equation (7), we see that the quadrature nodes are all the combinations of the eigenvalues, and the corresponding weights are products of inner products. More precisely, the quadrature is

$$(9) \quad \begin{aligned} & \int f(x) d\mathbb{P}(x) \\ & \approx \sum_{n_1=1}^S \sum_{n_2=1}^S \cdots \sum_{n_d=1}^S f(\lambda_{n_1}, \lambda_{n_2}, \dots, \lambda_{n_d}) e_0^\top u_{n_1} u_{n_1}^\top u_{n_2} u_{n_2}^\top \cdots u_{n_d} u_{n_d}^\top e_0 \\ & := \sum_{\mathbf{n} \in \mathbf{n}_{N,d}} w_{\mathbf{n}} f(\lambda_{\mathbf{n}}), \end{aligned}$$

where in the last line we compactly write the quadrature rules as

$$(10) \quad \begin{aligned} \lambda_{\mathbf{n}} & := [\lambda_{n_1} \ \lambda_{n_2} \ \cdots \ \lambda_{n_d}]^\top, \\ w_{\mathbf{n}} & := \langle e_0, u_{n_1} \rangle_S \left(\prod_{i=1}^{d-1} \langle u_{n_i}, u_{n_{i+1}} \rangle_S \right) \langle u_{n_d}, e_0 \rangle_S, \quad \langle x, y \rangle_S := x^\top y, \\ \mathbf{n}_{N,d} & := \{(1, 2, \dots, S) \times \cdots \times (1, 2, \dots, S)\}. \end{aligned}$$

If we let $d = 1$, it is clear that this generalised quadrature reduces to the unidimensional quadrature in Section 2. Furthermore, we show that this quadrature method is also exact for multivariate polynomials of degree equal to or less than $2N - 1$. This is given in the following lemma.

LEMMA 2. *The quadrature in Equation (9) is exact for every polynomial f of degree equal to or less than $2N - 1$.*

Proof. To show the exactness for polynomials of degree equal to or less than $2N - 1$, it is enough to prove $\langle \psi_{\mathbf{n}_0}, Z^{\mathbf{n}} \psi_{\mathbf{n}_0} \rangle = e_0^\top \mathring{H}_S^{\mathbf{n}} e_0$ for all $|\mathbf{n}| \leq 2N - 1$, where $Z^{\mathbf{n}} := \prod_{i=1}^d Z_i^{n_i}$ and $\mathring{H}_S^{\mathbf{n}} := \prod_{i=1}^d \mathring{H}_{S,i}^{n_i}$. Evidently, this holds for $|\mathbf{n}| = 0$. To prove this for $0 < |\mathbf{n}| \leq 2N - 1$, we decompose $\mathbf{n} = \mathbf{u} + \mathbf{v}$ in the way that $0 \leq |\mathbf{u}| \leq N - 1$ and $1 \leq |\mathbf{v}| \leq N$. By Parseval's identity we have

$$(11) \quad \begin{aligned} \langle \psi_{\mathbf{n}_0}, Z^{\mathbf{n}} \psi_{\mathbf{n}_0} \rangle & = \sum_{|\mathbf{q}| \geq 0} \langle \psi_{\mathbf{q}}, Z^{\mathbf{u}} \psi_{\mathbf{n}_0} \rangle \langle \psi_{\mathbf{q}}, Z^{\mathbf{v}} \psi_{\mathbf{n}_0} \rangle \\ & = \sum_{|\mathbf{q}| \leq N-1} \langle \psi_{\mathbf{q}}, Z^{\mathbf{u}} \psi_{\mathbf{n}_0} \rangle \langle \psi_{\mathbf{q}}, Z^{\mathbf{v}} \psi_{\mathbf{n}_0} \rangle, \end{aligned}$$

where we truncate the sum at $N - 1$ because of the orthonormality (i.e., $\langle \psi_{\mathbf{q}}, Z^{\mathbf{u}} \psi_{\mathbf{n}_0} \rangle = 0$ for $|\mathbf{q}| > N - 1$). Next we look at $\langle \psi_{\mathbf{q}}, Z^{\mathbf{v}} \psi_{\mathbf{n}_0} \rangle$ in Equation (11) for $|\mathbf{q}| \leq N - 1$

and $1 \leq |\mathbf{v}| \leq N$. We refer to the index of the first non-zero element of \mathbf{v} as i , that is, $v_j = 0$ for $j < i$, and $v_j \geq 0$ otherwise. Because $|\mathbf{v} - \mathbf{e}_i| \leq N - 1$, we can express the monomial $x \mapsto x^{\mathbf{v} - \mathbf{e}_i}$ as a linear combination of orthonormal polynomials up to order $N - 1$, that is, $x^{\mathbf{v} - \mathbf{e}_i} = \sum_{|\mathbf{p}| \leq N-1} c_{\mathbf{p}} \psi_{\mathbf{p}}(x)$ for some coefficients c . For finite matrix equivalent of the monomial of multiplication operators this means that

$$\begin{aligned}
(12) \quad \langle \psi_{\mathbf{q}}, Z^{\mathbf{v}} \psi_{\mathbf{n}_0} \rangle &= \langle Z_i \psi_{\mathbf{q}}, Z^{\mathbf{v} - \mathbf{e}_i} \psi_{\mathbf{n}_0} \rangle \\
&= \sum_{|\mathbf{p}| \leq N-1} c_{\mathbf{p}} \langle Z_i \psi_{\mathbf{q}}, \psi_{\mathbf{p}} \rangle = \sum_{|\mathbf{p}| \leq N-1} c_{\mathbf{p}} e_{j_{\mathbf{q}}}^{\top} \hat{H}_{S,i} e_{j_{\mathbf{p}}} \\
&= \sum_{|\mathbf{p}| \leq N-1} c_{\mathbf{p}} e_{j_{\mathbf{q}}}^{\top} \hat{H}_{S,i} \psi_{\mathbf{p}}(\hat{H}_S) e_0 = e_{j_{\mathbf{q}}}^{\top} \hat{H}_{S,i} \hat{H}_S^{\mathbf{v} - \mathbf{e}_i} e_0 = e_{j_{\mathbf{q}}}^{\top} \hat{H}_S^{\mathbf{v}} e_0,
\end{aligned}$$

where $j_{\mathbf{q}}$ and $j_{\mathbf{p}}$ depend on the ordering of the orthonormal basis functions so that $\psi_{\mathbf{q}}$ and $\psi_{\mathbf{p}}$ are the $j_{\mathbf{q}}$ -th and $j_{\mathbf{p}}$ -th basis function, respectively, both ranging from 0 to $S - 1$.

In order to preserve the ordering of the matrix computations in Equation (8), we further refine the decomposition to \mathbf{u} and \mathbf{v} so that there is index l such that $u_i = 0$ for $i > l$ and $v_j = 0$ for $j < l$. Now by Equation (12), we can write Equation (11) in terms of the finite matrices as

$$\langle \psi_{\mathbf{n}_0}, Z^{\mathbf{n}} \psi_{\mathbf{n}_0} \rangle = \sum_{|\mathbf{q}| \leq N-1} \langle \psi_{\mathbf{q}}, Z^{\mathbf{u}} \psi_{\mathbf{n}_0} \rangle \langle \psi_{\mathbf{q}}, Z^{\mathbf{v}} \psi_{\mathbf{n}_0} \rangle = \sum_{i=0}^{S-1} e_0^{\top} \hat{H}_S^{\mathbf{u}} e_i e_i^{\top} \hat{H}_S^{\mathbf{v}} e_0 = e_0^{\top} \hat{H}_S^{\mathbf{n}} e_0,$$

for all $0 < |\mathbf{n}| \leq 2N - 1$. \square

Based on the exactness for polynomials, we can then conclude the convergence of the quadrature method for continuous functions in the following proposition.

PROPOSITION 3. *Let the compact support of \mathbb{P} be a subset of a compact hypercube $D \subset \mathbb{R}^d$, and let $f: D \rightarrow \mathbb{R}$ be any continuous function. Recall that $S = \binom{N-1+d}{N-1}$. Then,*

$$(13) \quad \lim_{N \rightarrow \infty} \left| \int_D f \, d\mathbb{P} - \sum_{\mathbf{n} \in \mathbf{n}_{N,d}} w_{\mathbf{n}} f(\lambda_{\mathbf{n}}) \right| = 0.$$

Proof. Since the measure \mathbb{P} has support on D , the quadrature nodes $\{\lambda_{\mathbf{n}}\}_{\mathbf{n} \in \mathbf{n}_{N,d}}$ lie within D [31, Thm. 1]. By Stone–Weierstrass theorem, for any $\epsilon > 0$ there exists a polynomial ρ_{ϵ} on D such that $\sup_{x \in D} |f(x) - \rho_{\epsilon}(x)| < \epsilon$. Denote the residual $\tilde{f}_{\epsilon} := f - \rho_{\epsilon}$, and recall that $\{u_{n_i} u_{n_i}^{\top}\}_{i=1}^d$ are orthonormal projections. It follows that the Euclidean norm

$$\begin{aligned}
&\left\| \sum_{n_1=1}^S \sum_{n_2=1}^S \cdots \sum_{n_d=1}^S \tilde{f}(\lambda_{n_1}, \lambda_{n_2}, \dots, \lambda_{n_d}) u_{n_1} u_{n_1}^{\top} u_{n_2} u_{n_2}^{\top} \cdots u_{n_d} u_{n_d}^{\top} e_0 \right\|_2 \\
&\leq \sup_{x \in D} |\tilde{f}(x)| < \epsilon.
\end{aligned}$$

By Cauchy–Schwarz, the numerical quadrature of the residual \tilde{f} is bounded:

$$\begin{aligned}
|I_N(\tilde{f})| &:= \left| e_0^{\top} \sum_{n_1=1}^S \sum_{n_2=1}^S \cdots \sum_{n_d=1}^S \tilde{f}(\lambda_{n_1}, \lambda_{n_2}, \dots, \lambda_{n_d}) u_{n_1} u_{n_1}^{\top} u_{n_2} u_{n_2}^{\top} \cdots u_{n_d} u_{n_d}^{\top} e_0 \right| \\
&\leq \epsilon.
\end{aligned}$$

The exact integration of \tilde{f} is also bounded $I(\tilde{f}) := \int_D \tilde{f} d\mathbb{P} \leq \epsilon \mathbb{E}[\mathbf{1}_D]$. Recall that for any polynomial ρ_ϵ , we can always find an N_ϵ such that for every $N > N_\epsilon$, the numerical quadrature $I_N(\rho_\epsilon) = I(\rho_\epsilon)$ is exact. Therefore, we have

$$\begin{aligned} |I(f) - I_N(f)| &= |I(\tilde{f}) + I(\rho_\epsilon) - I_N(\tilde{f}) - I_N(\rho_\epsilon)| \\ &\leq |I(\tilde{f})| + |I_N(\tilde{f})| + |I(\rho_\epsilon) - I_N(\rho_\epsilon)| \leq (1 + \mathbb{E}[\mathbf{1}_D]) \epsilon. \end{aligned}$$

This concludes the limit in Equation (13). \square

As a summary, with given moments $M^N = \{m_{\mathbf{n}} : |\mathbf{n}| \leq 2N - 1\}$, we compute the quadrature rules as follows. We first select a partial order of the moments and the basis, and then we rearrange these moments into the Gram matrix G_S and the Hankel matrices $H_{S,1}, H_{S,2}, \dots, H_{S,d}$ (see, e.g., Example 1). Then, we orthonormalise these Hankel matrices as per Equation (6) to obtain $\hat{H}_{S,1}, \hat{H}_{S,2}, \dots, \hat{H}_{S,d}$. Finally, we compute the eigendecompositions of the orthonormalised Hankel matrices, and then combine the eigenvalues and eigenvectors as in Equation (10) for which we produce the quadrature rules. A pseudo-code of this quadrature method is given in the following algorithm.

Algorithm 1: d -dimensional moment quadrature with order N

```

1 Function moment_quadrature( $M^N$ ):
2   Build the Gram matrix  $G_S$  and Hankel matrices  $H_{S,1}, \dots, H_{S,d}$  based on
   the moments in  $M^N$ 
3   Cholesky decomposition  $L_S L_S^T = G_S$ 
4   for  $i = 1$  to  $d$  do                                     // In parallel
5      $\hat{H}_{S,i} = L_S^{-1} H_{S,i} (L_S^T)^{-1}$ 
6     Compute eigenvalues and eigenvectors  $\{\lambda_{n_i}, u_{n_i}\}_{n_i=1}^S$  of  $\hat{H}_{S,i}$ 
7   end
8   for  $\mathbf{n}$  in  $\mathbf{n}_{N,d}$  do                                       // In parallel
9      $\lambda_{\mathbf{n}} := [\lambda_{n_1} \ \lambda_{n_2} \ \dots \ \lambda_{n_d}]^T$ 
10     $w_{\mathbf{n}} := \langle e_0, u_{n_1} \rangle_S \left( \prod_{i=1}^{d-1} \langle u_{n_i}, u_{n_{i+1}} \rangle_S \right) \langle u_{n_d}, e_0 \rangle_S$ 
11  end
12  return  $\{w_{\mathbf{n}}, \lambda_{\mathbf{n}}\}_{\mathbf{n} \in \mathbf{n}_{N,d}}$ 
13 end

```

Figure 2 exemplifies three two-dimensional distributions and their corresponding quadrature rules with different order N . We see that the quadrature nodes are always confined within a rectangle area due to the Cartesian product construction, and that the weights are noticeably larger in the high-density areas of the distributions than the low-density areas. This suggests that the quadrature rules generated from the moments can represent these distributions well to a reasonable extent. However, we also observe from the figure that there are negative weights, since Equation (10) does not guarantee non-negativity of the product of the inner products. With negative weights, the discrete measures generated by the moments are signed. The negative weights may also result in numerical instabilities (e.g., the quadrature for positive integrands may become negative), but on the other hand, it follows from Proposition 3 that the sum of the negative weights admits an upper bound [23, Chap. 12.3, Thm. 8].

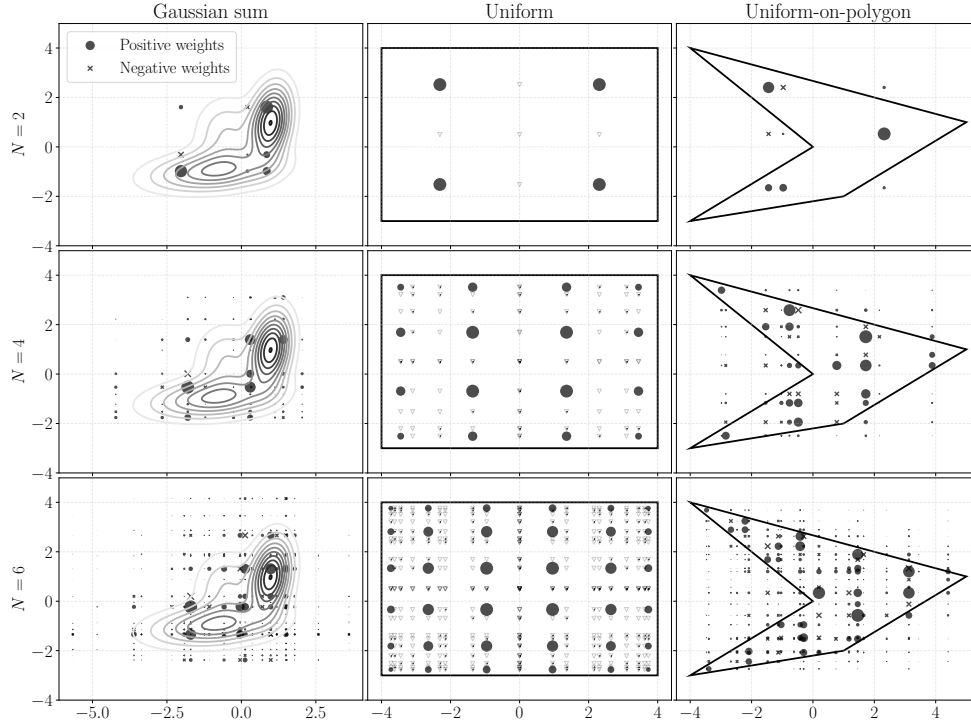


FIGURE 2. Quadrature rules for a Gaussian sum (left), a uniform (middle), and a uniform distribution on a polygon area (right). The location and size of the grey points represent the quadrature nodes and weights, respectively. For each plot, the sizes of the points are normalised by their maximum weight. In the middle, we mark the zero weights for the uniform distribution by triangles.

The uniform distribution in the middle of Figure 2 is an example that we can factorise the two-dimensional distribution into that of two independent random variables. We see that the majority of the nodes have zero weights, and that the nodes with non-zero weights agree with that of the product rule for independent variables [9, Chap. 5.6]. The product rule is commonly used for constructing multidimensional numerical integration rules, for instance, the multidimensional Gauss–Hermite quadrature used in Gaussian filters [17] and Edgeworth filters [5, 33]. Now our new method generalises the product rule to cases where it is impossible to factorise the joint probability distribution into independent ones (e.g., the left and right sides of Figure 2).

The quadrature method in its current form is computationally demanding for high-dimensional integrations. Recall that $S = \binom{N-1+d}{N-1}$, hence, if we fix d then $S \sim O(N^d / d!)$. Due to the Cartesian product construction, the number of quadrature nodes is of $O(N^{d^2} / (d!)^d)$ which grows polynomially in N of degree d^2 . If we instead fix N , then $S \sim O(d^{N-1} / (N-1)!)$, thus, the number of quadrature nodes grows faster than the exponential speed in d . There are a few ways to reduce the number of quadrature nodes, for instance, by using Lánczos iterations to solve the matrix-vector multiplications in Equation (9). It also makes sense to come up with a sparse version, since Figure 2 shows that there are plenty of insignificant weights, in particular when N is large. As an extreme example, if the probability distribution is elliptical and is thin along a direction, then the quadrature would be significantly inefficient, since

the quadrature nodes spread in a rectangle.

REMARK 4. *Using raw moments can lead to ill-conditioned Gram matrices [15]. To improve the condition number, we can make use of central or scaled moments. Specifically, if (w, λ) is a pair of quadrature weight and node generated by the raw moments M^N , then $(w, \sigma \lambda + \mu)$ is the corresponding pair of weight and node generated by the scaled central moment $\{\mathbb{E}[(X - \mu) / \sigma]^{\mathbf{n}} : |\mathbf{n}| \leq 2N - 1\}$, where μ and $\sigma \neq 0$ can be the mean and any scaling factor, respectively.*

3. Filtering with moment representation. Recall the definition of the filtering problem in Section 1 and the objectives that we aim to solve:

$$M_k^N := \{m_{k,\mathbf{n}} : |\mathbf{n}| \leq 2N - 1\},$$

$$m_{k,\mathbf{n}} := \mathbb{E}[X_k^{\mathbf{n}} | Y_{1:k}] := \int x^{\mathbf{n}} d\mathbb{P}_{X_k | Y_{1:k}}(x),$$

where $\mathbb{P}_{X_k | Y_{1:k}}$ is the filtering probability measure at time t_k . In this section, we apply the moment quadrature introduced in Section 2.1 to construct an approximation

$$\widehat{M}_k^N := \{\widehat{m}_{k,\mathbf{n}} : |\mathbf{n}| \leq 2N - 1\}, \quad m_{k,\mathbf{n}} \approx \widehat{m}_{k,\mathbf{n}},$$

such that $\widehat{m}_{k,\mathbf{n}}$ converges to $m_{k,\mathbf{n}}$ as $N \rightarrow \infty$ for any step k . Moreover, this algorithm is recursive in time in the way that the approximation \widehat{M}_k^N at t_k is only given by the previous approximation \widehat{M}_{k-1}^N at t_{k-1} and the current measurement Y_k . The recursion starts from the moments M_0^N of the initial \mathbb{P}_{X_0} which we know exactly. This filter is detailed as follows.

Suppose that at any time t_{k-1} we have the approximate (or exact) \widehat{M}_{k-1}^N of the true moments in M_{k-1}^N . The approximation must be valid in the sense that the Gram matrix built by the approximate moments is positive definite. Let us denote the quadrature rules generated by Algorithm 1 based on \widehat{M}_{k-1}^N as $\{w_{k-1,\mathbf{n}}, \lambda_{k-1,\mathbf{n}}\}_{\mathbf{n} \in \mathbf{n}_{N,d}}$. Then, we can propagate \widehat{M}_{k-1}^N through the SDE to approximate that of the measure $\mathbb{P}_{X_k | Y_{1:k-1}}$ at time t_k . Specifically, by Chapman–Kolmogorov equation, the moments

$$(14) \quad \int x^{\mathbf{n}} d\mathbb{P}_{X_k | Y_{1:k-1}}(x) = \int \mathbb{E}[X_k^{\mathbf{n}} | X_{k-1} = x] d\mathbb{P}_{X_{k-1} | Y_{1:k-1}}(x)$$

$$\approx \sum_{\mathbf{q} \in \mathbf{n}_{N,d}} w_{k-1,\mathbf{q}} \mathbb{E}[X_k^{\mathbf{n}} | X_{k-1} = \lambda_{k-1,\mathbf{q}}] := \overline{m}_{k,\mathbf{n}},$$

for all \mathbf{n} such that $|\mathbf{n}| \leq 2N - 1$, are approximated by $\overline{M}_k^N := \{\overline{m}_{k,\mathbf{n}} : |\mathbf{n}| \leq 2N - 1\}$. The conditional expectation $x \mapsto \mathbb{E}[X_k^{\mathbf{n}} | X_{k-1} = x]$ in the integral is the key that characterises the transition of the moments in time. However, the conditional expectation for the SDE is often intractable, and we have to find an approximation so as to evaluate the quadrature nodes.

One commonly used approximation is the Euler–Maruyama scheme (or other Gaussian-based approximations). By applying this scheme, we are approximating the conditional expectation $\mathbb{E}[X_k^{\mathbf{n}} | X_{k-1} = x]$ by the \mathbf{n} -moment of a multivariate Normal random variable with mean $x + a(x)(t_k - t_{k-1})$ and covariance $b(x)b(x)^{\top}(t_k - t_{k-1})$. The moment of such is analytically available by Isserlis’ theorem, however, its computational cost is astronomical (e.g., it needs at least $(|\mathbf{n}| - 1)!!$ summations over the covariance matrix elements). Although it is possible to significantly reduce the cost by Kan–Magnus method [20], the computation required is still an expensive

function of $|\mathbf{n}|$. Apart from the computational difficulty, it is also hard to improve the approximation error. As an example, computing the moment based on higher-order Itô–Taylor discretisations (e.g., Milstein) in closed form is possible only under limited conditions (e.g., diagonal dispersion b).

Provided that the SDE coefficients are sufficiently smooth, we can represent the conditional expectation by a J order Taylor moment expansion (TME) [36, 35]

$$(15) \quad \mathbb{E}[g(X_k) \mid X_{k-1} = x] = \sum_{j=0}^J (A^j g)(x) \frac{(t_k - t_{k-1})^j}{j!} + R(x, J, g, t_k, t_{k-1}),$$

$$(Ag)(x) := (\nabla_x g(x))^\top a(x) + \frac{1}{2} \text{tr} \left(b(x) b(x)^\top H_x g(x) \right),$$

by choosing $g(x) = x^{\mathbf{n}}$, where ∇_x and H_x denote the gradient and Hessian, respectively, A is the infinitesimal generator, and R is the remainder. If the time interval $t_k - t_{k-1}$ is not significantly large, we can discard R and use the truncated term as the approximation which converges as $J \rightarrow \infty$. The upside of this TME method is that the computation is scalable for approximating high-order moments. More precisely, unlike the Euler–Maruyama scheme, the number of calculations required in Equation (15) is independent of \mathbf{n} once we fix J . Although the equation has iterative gradients and Hessians, they are not difficult to implement with the help of automatic differentiations and Jacobian/Hessian-vector product solvers. The downside of this approach is that the approximate moments do not guarantee to form a positive definite Gram matrix, due to the truncation error.

We can then use \overline{M}_k^N to approximate that of $\mathbb{P}_{X_k \mid Y_{1:k}}$. By Bayes' rule, we apply the change-of-measure

$$(16) \quad \frac{d\mathbb{P}_{X_k \mid Y_{1:k}}}{d\mathbb{P}_{X_k \mid Y_{1:k-1}}}(x) = \frac{p_{Y_k \mid X_k}(Y_k \mid x)}{\int p_{Y_k \mid X_k}(Y_k \mid z) d\mathbb{P}_{X_k \mid Y_{1:k-1}}(z)},$$

thus, the \mathbf{n} -moment of $\mathbb{P}_{X_k \mid Y_{1:k}}$ is given by

$$(17) \quad m_{k,\mathbf{n}} = \frac{1}{h_k} \int x^{\mathbf{n}} p_{Y_k \mid X_k}(Y_k \mid x) d\mathbb{P}_{X_k \mid Y_{1:k-1}}(x),$$

$$h_k := \int p_{Y_k \mid X_k}(Y_k \mid x) d\mathbb{P}_{X_k \mid Y_{1:k-1}}(x),$$

which we can again approximate by applying the quadrature method. Specifically, let $\{\overline{w}_{k,\mathbf{n}}, \overline{\lambda}_{k,\mathbf{n}}\}_{\mathbf{n} \in \mathbf{n}_{N,d}}$ be the quadrature rules generated by \overline{M}_k^N , then the approximate moment for $\mathbb{P}_{X_k \mid Y_{1:k}}$ is

$$m_{k,\mathbf{n}} \approx \widehat{m}_{k,\mathbf{n}} := \sum_{\mathbf{q} \in \mathbf{n}_{N,d}} \overline{w}_{k,\mathbf{q}} (\overline{\lambda}_{k,\mathbf{q}})^{\mathbf{n}} p_{Y_k \mid X_k}(Y_k \mid \overline{\lambda}_{k,\mathbf{q}}) / \widehat{h}_k^N,$$

$$\widehat{h}_k^N := \sum_{\mathbf{n} \in \mathbf{n}_{N,d}} \overline{w}_{k,\mathbf{n}} p_{Y_k \mid X_k}(Y_k \mid \overline{\lambda}_{k,\mathbf{n}}).$$

With the approximate moments \widehat{M}_k^N , we can then compute the next \widehat{M}_{k+1}^N , and so forth for any step k by repeating this process.

Observe that $h_k = p_{Y_k \mid Y_{1:k-1}}(Y_k \mid Y_{1:k-1})$. Hence, the filtering routine simultaneously enables an approximation to the negative log-likelihood

$$(18) \quad \ell(Y_{1:k}) := -\log p_{Y_{1:k}}(Y_{1:k}) = -\sum_{j=1}^k \log h_k \approx -\sum_{j=1}^k \log \widehat{h}_j^N,$$

which we can use to estimate parameters in the filtering model by maximum likelihood. Moreover, the likelihood approximated by the filter is differentiable with respect to the model parameters. Hence, it is straightforward to leverage efficient gradient-based optimisation algorithms by means of automatic differentiations.

We summarise the filter with moment representations in the following algorithm.

Algorithm 2: Moment filter

Inputs: Order N , measurements $Y_{1:T}$, and initial moments M_0^N
Outputs: Moments $\widehat{M}_1^N, \widehat{M}_2^N, \dots, \widehat{M}_T^N$ and negative log-likelihood $\widehat{\ell}$

```

1  $\widehat{M}_0^N = M_0^N$ 
2  $\widehat{\ell} = 0$ 
3 for  $k = 1$  to  $T$  do
    // Prediction step
4    $\{w_{k-1,\mathbf{n}}, \lambda_{k-1,\mathbf{n}}\}_{\mathbf{n} \in \mathfrak{n}_{N,d}} = \text{moment\_quadrature}(\widehat{M}_{k-1}^N)$ 
5   for  $\mathbf{n}: |\mathbf{n}| \leq 2N - 1$  do // In parallel
6      $\overline{m}_{k,\mathbf{n}} = \sum_{\mathbf{q} \in \mathfrak{n}_{N,d}} w_{k-1,\mathbf{q}} \mathbb{E}[X_k^{\mathbf{n}} | X_{k-1} = \lambda_{k-1,\mathbf{q}}]$ 
7   end
8    $\overline{M}_k^N = \{\overline{m}_{k,\mathbf{n}}: |\mathbf{n}| \leq 2N - 1\}$ 
    // Update step
9    $\{\overline{w}_{k,\mathbf{n}}, \overline{\lambda}_{k,\mathbf{n}}\}_{\mathbf{n} \in \mathfrak{n}_{N,d}} = \text{moment\_quadrature}(\overline{M}_k^N)$ 
10   $\widehat{h}_k^N = \sum_{\mathbf{n} \in \mathfrak{n}_{N,d}} \overline{w}_{k,\mathbf{n}} p_{Y_k | X_k}(Y_k | \overline{\lambda}_{k,\mathbf{n}})$ 
11  for  $\mathbf{n}: |\mathbf{n}| \leq 2N - 1$  do // In parallel
12     $\widehat{m}_{k,\mathbf{n}} = \sum_{\mathbf{q} \in \mathfrak{n}_{N,d}} \overline{w}_{k,\mathbf{q}} (\overline{\lambda}_{k,\mathbf{q}})^{\mathbf{n}} p_{Y_k | X_k}(Y_k | \overline{\lambda}_{k,\mathbf{q}}) / \widehat{h}_k^N$ 
13  end
14   $\widehat{\ell} = \widehat{\ell} - \log \widehat{h}_k^N$ 
15   $\widehat{M}_k^N = \{\widehat{m}_{k,\mathbf{n}}: |\mathbf{n}| \leq 2N - 1\}$ 
16 end
```

3.1. Computational complexity. As shown in Algorithm 2, the moment filter is a sequential algorithm in time, hence, the time complexity is linear in the number of measurements T . At each filtering step, the computation cost is dominated by either the Cholesky decomposition of the Gram matrix (of size $S \times S$), or summing over the quadrature evaluations (of length S^d) depending on the actual implementation. If the summation is implemented schoolbook sequentially, then the summation complexity is $O(S^d)$ which is greater than that of the Cholesky decomposition if $d > 3$. On the other hand, if the summation is implemented in parallel, then the cost of the Cholesky decomposition dominates, which is $O(S^3)$. At every step, the filter computes the summation and Cholesky decomposition three and two times, respectively. Overall, Algorithm 2 has time complexity

- $O(2TS^3)$, if the summation is implemented in parallel,
- $O(2TS^3)$, if the summation is implemented sequentially and $d \leq 3$, or
- $O(3TS^d)$, if the summation is implemented sequentially and $d > 3$.

Recall that $S = \binom{N-1+d}{N-1}$, and that $S \sim O(N^d/d!)$ if we fix the dimension d . Therefore, the time complexity of the filter is polynomial in the order N , and the degree of the polynomial is determined by the state dimension and the actual implementation

of the filter.

The time complexity of the filter is not significantly impacted by the measurement variable dimension d_y . At each step k , the filter evaluates the measurement density function $x \mapsto p_{Y_k | X_k}(Y_k | x)$ by the quadrature nodes. The complexity of each evaluation depends on d_y , for example, $O(d_y^3)$ for multivariate Normal distributions. But on the other hand, these evaluations are independent which can be done in parallel, hence, the complexity is not multiplied by the number of quadrature nodes. In practice, d_y is far less than S when the order N is large.

3.2. Convergence analysis. We aim to show that the moment filter converges in both moments and distribution as $N \rightarrow \infty$ at every filtering step. This is intuitive, since the moment quadrature that we use is exact for polynomials of degree equal to or less than $2N - 1$. If additionally the limiting distribution is determined by its moments, then the approximation converges in distribution too followed by the method of moments.

Recall that the filter is a recursive chain of approximations. Therefore, if we can prove that for any fixed step $k-1$ the convergence of \widehat{M}_{k-1}^N to $\mathbb{P}_{X_{k-1} | Y_{1:k-1}}$ implies the convergence of \widehat{M}_k^N to $\mathbb{P}_{X_k | Y_{1:k}}$, then by mathematical induction the filter converges at every step as long as the initial moments converges to \mathbb{P}_{X_0} . To keep the results clean, let us use shorthand $I_\mu(f) := \int f d\mu$, and denote δ_x the Dirac measure at any point x . If a measure μ converges weakly and in moments to another measure ν , then we denote $\mu \xrightarrow{\text{w.m.}} \nu$. All the probability measures/distributions in this section operate on the same canonical space $(\mathbb{R}^d, \mathcal{B}(\mathbb{R}^d))$, where \mathcal{B} stands for the Borel sigma-algebra. Then, we make the following lemma that backbones the filtering convergence for any fixed step.

LEMMA 5. *Let μ and ν be two probability measures such that 1) ν is determined by its moments; 2) for any monomial $\eta_{\mathbf{n}}$, there is a bounded continuous, or polynomial function $g_{\eta_{\mathbf{n}}}$ that $I_\nu(\eta_{\mathbf{n}}) = I_\mu(g_{\eta_{\mathbf{n}}})$. Let $\widehat{\mu}_N$ be any finite measure that $\widehat{\mu}_N \xrightarrow{\text{w.m.}} \mu$ as $N \rightarrow \infty$, and suppose that the Gram matrix generated by $\mathcal{M}^N := \{I_{\widehat{\mu}_N}(g_{\eta_{\mathbf{n}}}) : |\mathbf{n}| \leq 2N - 1\}$ is positive definite for all N . Then the measure $\widehat{\nu}_N := \sum_{\mathbf{n} \in \mathfrak{n}_{N,d}} w_{\mathbf{n}} \delta_{\lambda_{\mathbf{n}}} \xrightarrow{\text{w.m.}} \nu$ as $N \rightarrow \infty$, where $\{w_{\mathbf{n}}, \lambda_{\mathbf{n}}\}_{\mathbf{n} \in \mathfrak{n}_{N,d}}$ are the quadrature rules generated by \mathcal{M}^N .*

Proof. Since $\widehat{\mu}_N$ converges weakly and in moments to μ , we have for any monomial $\eta_{\mathbf{n}}$ the expectation $I_{\widehat{\mu}_N}(g_{\eta_{\mathbf{n}}}) \rightarrow I_\mu(g_{\eta_{\mathbf{n}}})$ as $N \rightarrow \infty$. Therefore, the approximate moment $I_{\widehat{\mu}_N}(g_{\eta_{\mathbf{n}}})$ converges to the true moment $I_\nu(\eta_{\mathbf{n}})$ of ν for all \mathbf{n} . By the definition of the quadrature method, the moment of $\widehat{\nu}_N$ is

$$I_{\widehat{\nu}_N}(\eta_{\mathbf{n}}) = \begin{cases} I_{\widehat{\mu}_N}(g_{\eta_{\mathbf{n}}}) \in \mathcal{M}^N, & |\mathbf{n}| \leq 2N - 1, \\ \sum_{\mathbf{q} \in \mathfrak{n}_{N,d}} w_{\mathbf{q}} \eta_{\mathbf{n}}(\lambda_{\mathbf{q}}) < \infty, & |\mathbf{n}| > 2N - 1, \end{cases}$$

which is finite for all \mathbf{n} and N . Hence, for any fixed \mathbf{n} , we can always find a large enough N such that $I_{\widehat{\nu}_N}(\eta_{\mathbf{n}}) = I_{\widehat{\mu}_N}(g_{\eta_{\mathbf{n}}})$, and that $I_{\widehat{\nu}_N}(\eta_{\mathbf{n}}) \rightarrow I_\nu(\eta_{\mathbf{n}})$ as $N \rightarrow \infty$. This proves that $\widehat{\nu}_N$ converges in moment to ν . It is then followed by Fréchet–Shohat theorem [13, pp. 540] that the measure $\widehat{\nu}_N$ converges weakly to ν as well. \square

The convergence of the moment filter is then a result of iterative applications of Lemma 5. This result is concluded in Proposition 10 under the following model assumptions.

ASSUMPTION 6. *The distributions \mathbb{P}_{X_0} , $\mathbb{P}_{X_k | Y_{1:k}}$, and $\mathbb{P}_{X_k | Y_{1:k-1}}$ for $k \geq 1$ are determined by their moments.*

ASSUMPTION 7. *The initial approximation $\widehat{\mathbb{P}}_{X_0}^N := \sum_{\mathbf{n} \in \mathbf{n}_{N,d}} w_{k,\mathbf{n}} \delta_{\lambda_{k,\mathbf{n}}} \xrightarrow{\text{w.m.}} \mathbb{P}_{X_0}$.*

ASSUMPTION 8. *For every \mathbf{n} , the function $x \mapsto \mathbb{E}[X_k^{\mathbf{n}} | X_{k-1} = x]$ is bounded and continuous, or polynomial. Almost surely for every \mathbf{n} and k , the functions $x \mapsto p_{Y_k | X_k}(\cdot | x)$ and $x \mapsto x^{\mathbf{n}} p_{Y_k | X_k}(\cdot | x)$ are bounded and continuous, or polynomial.*

ASSUMPTION 9. *For all $N \geq 1$ and $k \geq 0$, the Gram matrices generated by the moments in \widehat{M}_k^N and \overline{M}_k^N are positive definite.*

PROPOSITION 10. *Suppose that Assumptions 6 to 9 are satisfied. Then almost surely for every $k \geq 0$,*

$$(19) \quad \widehat{\mathbb{P}}_{X_k | Y_{1:k}}^N \xrightarrow{\text{w.m.}} \mathbb{P}_{X_k | Y_{1:k}},$$

as $N \rightarrow \infty$, where $\widehat{\mathbb{P}}_{X_k | Y_{1:k}}^N := \sum_{\mathbf{n} \in \mathbf{n}_{N,d}} w_{k,\mathbf{n}} \delta_{\lambda_{k,\mathbf{n}}}$ is the discrete measure given by the moments \widehat{M}_k^N . Moreover, the approximate likelihood $\widehat{h}_k^N \rightarrow h_k$ almost surely.

Proof. Assumption 7 implies that Equation (19) holds for $k = 0$ by definition. Suppose that $\widehat{\mathbb{P}}_{X_{k-1} | Y_{1:k-1}}^N \xrightarrow{\text{w.m.}} \mathbb{P}_{X_{k-1} | Y_{1:k-1}}$ for any $k > 1$. Then by Equation (14) we have the relation

$$I_{\mathbb{P}_{X_k | Y_{1:k-1}}}(\eta_{\mathbf{n}}) = I_{\mathbb{P}_{X_{k-1} | Y_{1:k-1}}}(g_{\eta_{\mathbf{n}}}),$$

by taking $g_{\eta_{\mathbf{n}}}(x) = \mathbb{E}[X_k^{\mathbf{n}} | X_{k-1} = x]$. Hence, Lemma 5 concludes that the measure $\sum_{\mathbf{n} \in \mathbf{n}_{N,d}} \overline{w}_{k,\mathbf{n}} \overline{\delta}_{\lambda_{k,\mathbf{n}}} \xrightarrow{\text{w.m.}} \mathbb{P}_{X_k | Y_{1:k}}$, and this holds almost surely. It follows that $\widehat{h}_k^N \rightarrow h_k$ almost surely. Next, Equation (16) similarly indicates the relation $I_{\mathbb{P}_{X_k | Y_{1:k}}}(\eta_{\mathbf{n}}) = I_{\mathbb{P}_{X_k | Y_{1:k-1}}}(g_{\eta_{\mathbf{n}}})$ by taking $g_{\eta_{\mathbf{n}}}(x) = x^{\mathbf{n}} p_{Y_k | X_k}(Y_k | x) / h_k$. Hence, by applying Lemma 5 again, we have $\widehat{\mathbb{P}}_{X_k | Y_{1:k}}^N \xrightarrow{\text{w.m.}} \mathbb{P}_{X_k | Y_{1:k}}$. The statement of the proposition is then concluded by induction. \square

The proposition above shows that the moment filter is asymptotically convergent under a few assumptions on the system. Assumptions 6 and 7 are not restrictive, since there are a large class of distributions determined by moments (see sufficient conditions in e.g., [21, Chap. 15]). Assumption 8 asks the integrands used in the moment filter be either bounded continuous or polynomial, since the convergence in both distribution and moments directly implies the convergence of such expectations. A trivial example that satisfies this assumption is any linear Gaussian system. It is possible to generalise Assumption 8 for analytical functions as well, if the dominated convergence theorem applies for every order power series expansion of the integrand.

Assumption 9 can be ambiguous, since it does not explicitly clarify what types of systems can guarantee the moment matrices be positive definite. But on the other hand, it is fundamentally hard for any quadrature method to ensure the approximate moments be jointly valid (e.g., Monte Carlo). One solution to this problem is to introduce another approximation on top of the system. For instance, we can approximate the transition $\mathbb{E}[X_k^{\mathbf{n}} | X_{k-1} = x]$ by Euler–Maruyama, so that each quadrature evaluation gives a Gaussian moment which is always valid by definition. Another solution, but numerically, is to use LDL decomposition instead of Cholesky, and then clip the non-positive diagonal elements to small epsilons [6]. This amounts to a moment-matrix completion by finding a new set of valid moments that are nearest (in Frobenius norm) to the approximate moments.

REMARK 11. *It is important to remark that Lemma 5 is independent of our quadrature methods introduced in Section 2. Specifically, the lemma holds for any moment-*

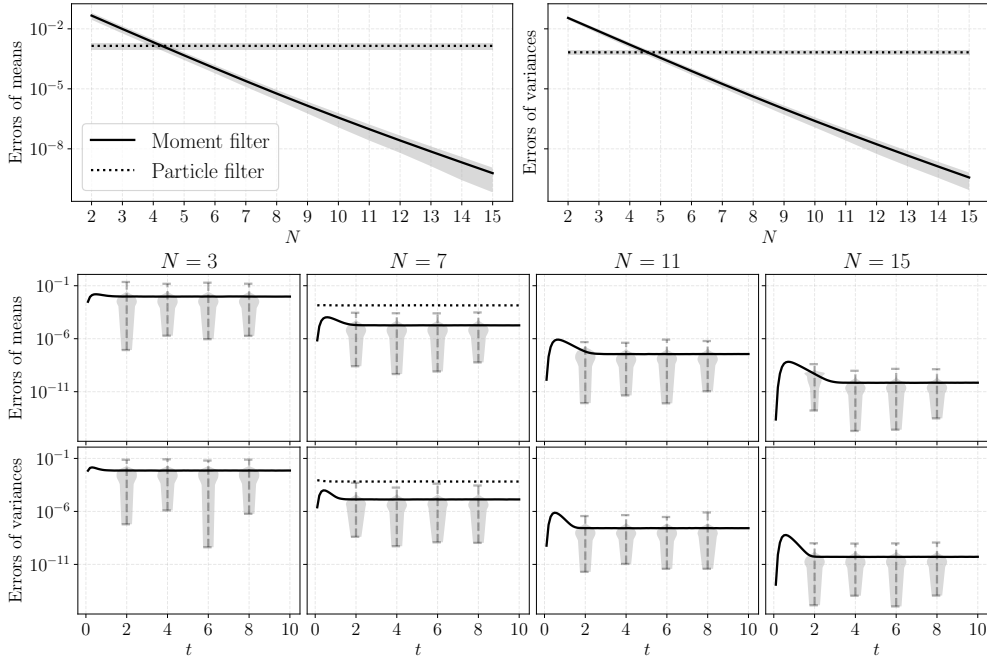


FIGURE 3. The filtering absolute errors (in log scale) for the model in Equation (20). The two figures in the first row show the errors as functions of the order N , where at each N we average the errors over time, and then we plot the mean and two-standard deviation (i.e., the shaded area) from the MC simulations. The eight figures in the bottom two rows show the errors as functions of the time t , where we fix four N . The shaded violin plots show the distribution of the MC runs, with the dashed whiskers showing the extrema, and the solid black lines showing the means. The dotted lines show the mean errors of the particle filter for comparison.

based quadrature, as long as it gives finite approximations and exact integrations for monomials of a degree determined by N . As a consequence, the convergence of the moment filter does not break if we replace the moment-quadrature with any such.

4. Experiments. In this section, we conduct four experiments to numerically show the convergence of the moment filter, and to compare the performance against other commonly used filters. For numerical stability, we use central moments instead of raw moments in all the experiments (see, Remark 4). For approximating the conditional expectation in Equation (14), we use the Taylor moment expansion of order three. All the experiments are implemented in the JAX of Python, and the implementations are published at <https://github.com/zgbkdlm/mfs> for reproducibility.

4.1. Numerical convergence. To numerically show that the moment filter is convergent as $N \rightarrow \infty$, we test the filter on a linear Gaussian model

$$(20) \quad \begin{aligned} dX(t) &= -\frac{1}{\ell} X(t) dt + \sqrt{\frac{2\sigma^2}{\ell}} dW(t), & X(0) &\sim \mathcal{N}(0, \sigma^2), \\ Y_k &= X_k + \xi_k, & \xi_k &\sim \mathcal{N}(0, 1), \end{aligned}$$

where we fix the SDE parameters to $\ell = 1$ and $\sigma = 0.5$. The reason for using this model is that we can exactly compute the true filtering distribution by a Kalman filter. To

test the convergence statistically, we conduct 10,000 independent Monte Carlo (MC) simulations. For each MC simulation, we generate 100 measurements Y_1, Y_2, \dots, Y_{100} at evenly placed times $t_1 = 0.1, t_2 = 0.2, \dots, t_{100} = 100$, respectively, then we compute the absolute errors of the filtering means and variances of the filter. More specifically, the two absolute errors are $|\hat{m}_{k,1} - \mathbb{E}[X_k | Y_{1:k}]|$ and $|\hat{v}_k - \text{Var}[X_k | Y_{1:k}]|$ for $k = 1, 2, \dots, 100$, where $\hat{m}_{k,1}$ and \hat{v}_k are the approximate filtering mean and variance, respectively.

Furthermore, we apply a standard particle filter with 100,000 particles for comparison of the convergence. We use the stratified resampling at every step, and use the variance-optimal distribution [7, Thm. 10.1] as the proposal which is available in closed form for this model.

The results are shown in Figure 3. From the first row of the figure, we see that the moment filtering error decreases as N increases. Moreover, the convergence speed is numerically almost linear in the log scale, implying that the actual convergence speed is possibly a high degree polynomial of N . At $N = 5$, the error of the moment filter starts to be better than that of the particle filter. On top of that, the moment filter with $N = 5$ requires only 5 quadrature nodes and 10 moments, while the particle filter has 100,000 particles. When $N = 15$, the convergence of the moment filter outperforms the particle filter out of a number of orders of magnitudes, while the actual running time of the moment filter is still faster than that of the particle filter.

The bottom two rows in Figure 3 show the mean absolute errors as functions of time for a few fixed N . We see that at the initial time the errors are small, and then the errors increase as t increases. This is true, since we know the exact moments of the initial random variable, and the moment filter by definition accumulates the filtering errors in time. However, we also observe that the errors shortly stop to increase (e.g., at $t \approx 1$) and stabilise at certain levels. This suggests that the moment filter may have a bounded stability property which is worth investigating in future works.

4.2. Beneš–Bernoulli. We next test the convergence of the moment filter with a non-linear SDE and Bernoulli binary measurements:

$$(21) \quad \begin{aligned} dX(t) &= \tanh(X(t)) dt + dW(t), \quad X(0) \sim \frac{1}{2}(\mathcal{N}(-0.5, 0.05) + \mathcal{N}(0.5, 0.05)), \\ Y_k | X_k &\sim \text{Bernoulli}\left(\frac{1}{1 + \exp(-X_k^2/5)}\right), \end{aligned}$$

whose filtering distribution is multimodal. For this model, it is hard to derive the exact solution analytically, but since the state is unidimensional, we can numerically compute the true solution by brute force up to machine precision. Specifically, we numerically compute the filtering PDFs (see, [30, Algorithm 10.15]) and their characteristic functions by trapezoidal rules at 2,000 spatial grids over a finite horizon where the true solution lies in.

We compare the moment filter to a bootstrap particle filter (10,000 samples with stratified resampling) and a Gaussian filter with Gauss–Hermite quadrature (of order 11). It is interesting to remark that the extended Kalman filters by definition do not work for this model, because the non-linear function in the Bernoulli parameter gives zero Kalman gain at the origin. Hence we do not compare to extended Kalman filters.

We compute the approximation errors for the characteristic function of the filtering distribution. Denote $\varphi_k(z) := \mathbb{E}[\exp(izX_k) | Y_{1:k}]$ as the true characteristic function, and $\hat{\varphi}_k$ as the approximate. Then the error metric we use is $\sup_{z \in [-\gamma, \gamma]} |\varphi_k(z) - \hat{\varphi}_k(z)|$, where $\gamma = 2$. For the moment filter and particle filter, we use its mo-

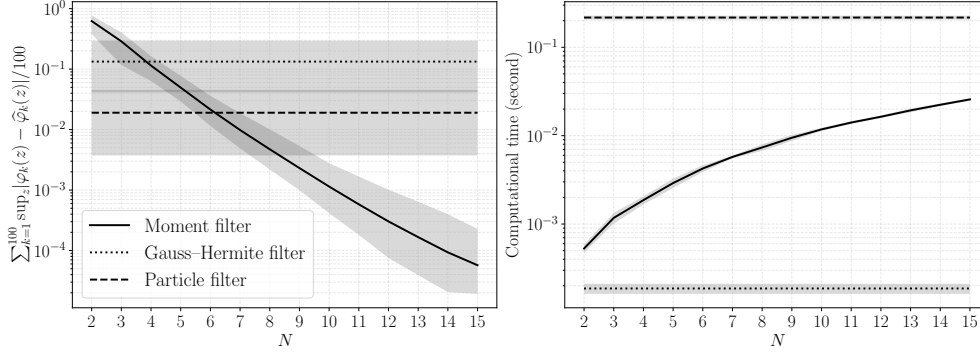


FIGURE 4. The estimation errors (left) and running times (right) of the filters for the Beneš–Bernoulli model in Equation (21). The shaded area plots the 0.95 quantile region computed from the 1,000 MC simulations.

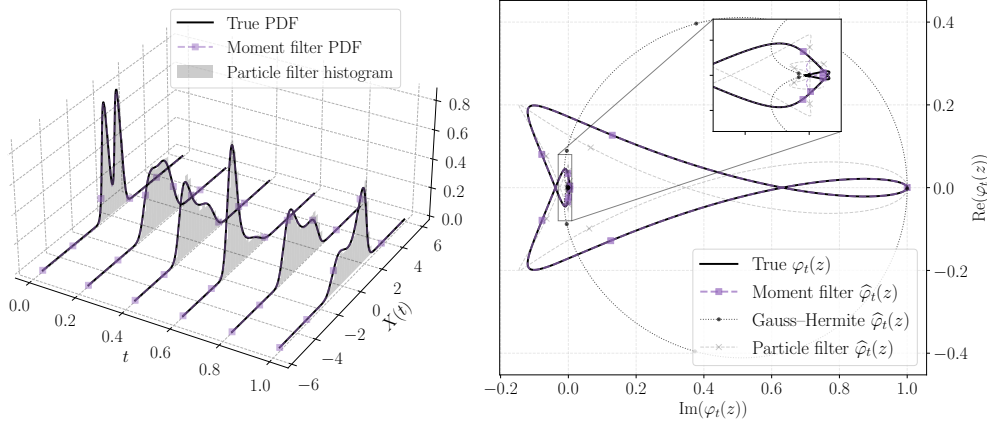


FIGURE 5. Demonstration of the filtering for the Beneš–Bernoulli model in Equation (21), with a fixed realisation of measurements. The left figure shows the evolution of the filtering PDFs. The right figure shows the characteristic functions at $t = 0.8$ with $z \in [-9, 9]$. The PDF of the moment filter is numerically computed by the Fourier transform of the estimated characteristic function. The moment filter in this figure uses $N = 15$, and its results overlap with the truth visually.

ments and samples, respectively to compute their approximate $\hat{\varphi}_k$. For the Gauss–Hermite filter, its approximate characteristic function is given by that of the Normal distribution. To average the errors, we use 1,000 independent MC simulations, and in each simulation, we generate 100 measurements at evenly placed times $t_1 = 0.01, t_2 = 0.02, \dots, t_{100} = 1$. Alongside the errors, we also present the running times of the filters. The running times are computed on a personal computer with Intel i9-10900K CPU.

The estimation errors are shown on the left side of Figure 4. We see that error of the moment filter is large when using low order of moments $N = 2$. However, the error decreases in a near-linear speed (in log-scale) as we increase N , similar to the results in Section 4.1. At around $N = 4$ and $N = 6$, the error of the moment filter starts to be better than the Gauss–Hermite filter and particle filter, respectively.

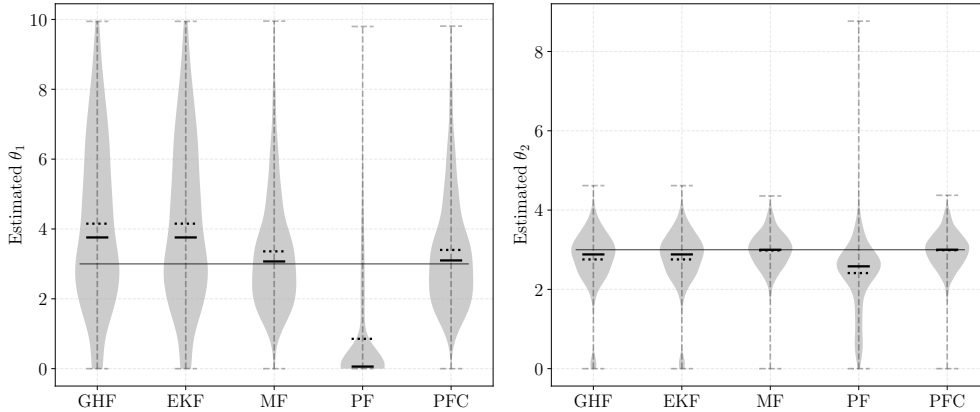


FIGURE 6. Estimates parameters for the model in Equation (22). The grey violin plots show the distributions of the estimated parameters in all the MC runs, with the dashed whiskers representing the extrema. The solid and dotted black lines show the medians and means, respectively. The strike-through black lines represent the true parameter values. Moreover, in the 1,000 MC runs, GHF, EKF, MF, PF, and PFC have 105, 105, 34, 442, and 18 divergences, respectively.

Meanwhile, as we increase N , the deviation of the moment filter error (i.e., the shaded area) enlarges too, but the deviation is smaller than other filters for most N .

The running times of the filters are shown in the right side of Figure 4. We see that the Gauss–Hermite filter and particle filter are the fastest and slowest, respectively, with the moment filter in between the two. As we increase N , the speed of the moment filter decreases, but the decreasing speed is sub-linear (in log-scale). This is true, because the time complexity of the unidimensional moment filter is cubic in N (see, Section 3.1). At $N = 15$, the accuracy of the moment filter is significantly better than the particle filter, while the speed is around ten times faster too.

In Figure 5, we demonstrate one simulation from the MC runs, and then plot the filtering PDF and characteristic function estimates. On the left figure, we see that the true PDFs are significantly non-Gaussian, while the estimated PDFs follow well the true PDFs. However, it is hard to see the differences between the moment filter and particle filter estimates. Hence, on the right figure, we plot the estimates for the characteristic function at $t = 0.8$ which shows the difference more clearly. We find from the figure that the moment filter estimate is the closest to the truth, even at the tail around $|z| = 9$. On the other hand, the Gauss–Hermite filter’s estimate is largely off, since it uses the Gaussian approximation. The particle filter has a better estimate than Gauss–Hermite, but its estimate deviates significantly from the truth compared to that of the moment filter.

It is worth noting that the quadrature method in Section 2 with $N = 2$ is equivalent to Gauss–Hermite (GH) of order two when $d = 1$. However, this does not mean that the moment filter with $N = 2$ is the same as a Gaussian filter with GH of order two. The GH filter approximates the filtering distribution by Gaussian, while the moment filter does not. The two filters differ in computing Equations (14) and (17), hence, they do not give the same results in Figure 4 at $N = 2$.

4.3. Parameter estimation. In this section we test the parameter estimation by minimising the negative log-likelihood produced by the filters (e.g., Equation (18)).

The test model is

$$\begin{aligned}
 dX(t) &= X(t) (1 - \theta_1 X(t)^2) dt + dW(t), \\
 X(0) &\sim \frac{1}{2}(\mathcal{N}(-0.5, 0.05) + \mathcal{N}(0.5, 0.05)), \\
 Y_k | X_k &\sim \text{Poisson}\left(\log(1 + \exp(\theta_2 X_k))\right),
 \end{aligned}
 \tag{22}$$

where the parameters are set to be $\theta_1 = \theta_2 = 3$. To minimise the objectives, we use an L-BFGS-B optimiser with a positive bijection $x \mapsto \log(\exp(x)+1)$ over the parameters which ensures positive estimates. The gradients with respect to the parameters are obtained by automatic differentiation. The initial values for the two parameters are uniformly set to be 0.1.

We conduct 1,000 independent MC runs, and in each MC run we generate 1,000 measurements at times $t_1 = 0.01, t_2 = 0.02, \dots, t_{1000} = 10$. In addition, if the optimiser numerically diverges, or the estimated parameters exceed the threshold 10, then we mark the corresponding run as divergent. For comparison, we test the moment filter with $N = 7$ against the Gauss–Hermite filter (GHF), the extended Kalman filter (EKF), and the bootstrap particle filter (PF). The configurations of these filters are the same as in Section 4.2. However, the gradient produced by the PF with the standard resampling methods is biased. Hence, for a fair comparison, we use the continuous resampling method in [8] to compensate such biasedness. We abbreviate this particle filter with continuous resampling as PFC.

The distribution of the estimated parameters are shown in Figure 6. We see that the estimates of the moment filter are evidently closest to the truth. In particular for θ_1 , the distribution of the moment filter estimates is more concentrated around the truth and is less tailed, compared to GHF and EKF. Moreover, for θ_2 , GHF and EKF have a few runs that give near-zero estimates, but, this problem does not appear for the moment filter. Among all the filters, PF is numerically the worst, as it does not give reasonable estimates for θ_1 , and the estimates for θ_2 have large extrema and are heavily tailed. The performance of PFC is comparable to the moment filter, at the cost of using the continuous resampling.

In all the 1,000 MC runs, GHF, EKF, MF, PF, and PFC have 105, 105, 34, 442, and 18 divergences, respectively. This shows that the moment filter is relatively stable for this parameter estimation task compared to other filters.

4.4. Prey-predator. To test the performance of the moment filter for multidimensional systems, we consider the following prey-predator model

$$\begin{aligned}
 dX^{(1)}(t) &= X^{(1)}(t) (\alpha - \beta X^{(2)}(t)) dt + \sigma X^{(1)}(t) dW^{(1)}(t), \\
 dX^{(2)}(t) &= X^{(2)}(t) (\zeta X^{(1)}(t) - \gamma) dt + \sigma X^{(2)}(t) dW^{(2)}(t), \\
 Y_k | X_k &\sim \text{Poisson}\left(1 / (1 + \exp(-(X_k^{(1)})^3 + 1))\right),
 \end{aligned}
 \tag{23}$$

where $\alpha = \beta = \zeta = \gamma = 4$, and $\sigma = 0.1$. The prey-predator equation is commonly used by computational ecologist for modelling population growth, where $X^{(1)}$ and $X^{(2)}$ represent the populations of the preys and predators, respectively. To ensure the states be positive, we let the initial distribution of the SDE be a Normal with mean ones and small diagonal covariance scaled by 10^{-3} . We simulate this model with 10,000 MC runs at 2,000 times $t_1 = 0.001, t_2 = 0.002, \dots, t_{2000} = 2$. However, for this model it is hard to compute the true filtering solution. Hence, we instead compute the projection error $\mathbb{E}[\|X(t_k) - \hat{m}_{k,1}\|_1]$ at every time t_k , where $\hat{m}_{k,1}$ is the

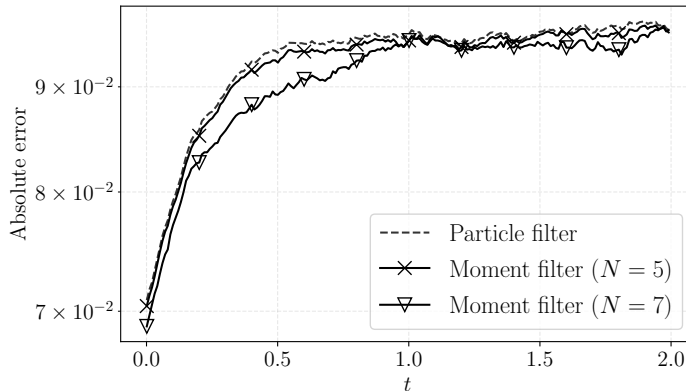


FIGURE 7. The estimation absolute errors for the prey-predator model in Equation (23).

estimated filtering mean, and $\|\cdot\|_1$ is the absolute norm. We use the same particle filter as in the previous section, for comparison.

The results are shown in Figure 7. We see that the moment filter with $N = 5$ is already slightly better than the particle filter. With $N = 7$, the moment filter outperforms the particle filter. In average, the particle has absolute error 9.21×10^{-2} , while the moment filter with $N = 5$ and $N = 7$ have error 9.15×10^{-2} and 9.03×10^{-2} , respectively. However, we remark that in all the 10,000 MC runs, the moment filter numerically diverges 909 and 4,746 times for $N = 5$ and $N = 7$, respectively. The filter diverges because the Gram matrices generated by the moments are numerically not positive definite. As a contrast, all the particle filter runs are stable. This shows that although the moment filter is more performant than the particle filter, the moment filter can be numerically unstable depending on the model.

5. Conclusions. In this paper, we have developed a stochastic filter that represents the filtering distributions by approximate moments. Moreover, we proved that this filter is asymptotically exact, in the sense that the approximation converges to the truth in both distribution and moments, in the number of moments used. To make the moment filter computable, we have also developed a moment-based quadrature method based on the finite-matrix representation of multiplication operators. Our experiments showed that the moment filter numerically converges to the true solutions, and the filter outperforms a number of commonly used filters in terms of both computation time and estimation error.

We would also like to remark the limitation of the method for high-dimensional systems. As shown in Section 3.1, the computational complexity of the moment filter does not scale well in the state dimension, due to the Cartesian-product construction of quadrature rules. But on the other hand, as we have mentioned in Remark 11, the convergence of the moment filter is independent of the used quadrature method. Hence, to reduce the computation, we can replace the moment quadrature with any that is more efficient, for example, by introducing a sparse version of Algorithm 2. It is reasonable to come up with a sparse routine, since from Figure 2 we evidently see plenty of quadrature weights that are too small to be useful. Another problem for high-dimensional systems is the numerical stability. As shown in the experiment in Section 4.4, the moment filter can numerically diverge due to non-positive-definite Gram matrices. This problem can be numerically solved by modified

Cholesky decompositions to certain extent, but it is unclear whether this breaks the convergences. Therefore, developing a more efficient and numerical stable moment quadrature method is an important topic for future investigations.

The convergence analysis in Section 3.2 proves that the moment filter converges, but it does not explicitly quantify the approximation error. For future works, it is interesting to measure how the error accumulates in time, and also to see if the error has a finite bound. Figure 3 numerically shows that the error has a finite bound for a specific model.

6. Related works. The essence of the paper consists in representing the filtering distributions by a sequence of moments. On the special case of continuous-time measurements, this idea translates into projecting the Kushner–Stratonovich equation solution onto a finite-dimensional basis spanned by the moments. As an example, in [24, Equ. 15] and [4, Sec. 7] they show a system of differential equations of moments, so that we can approximately compute the moments by simulating the moment equations. These moment equations, however, have intractable expectations, hence, they in addition approximate the filtering distributions by, for instance, Gaussian [24] or exponential families [4]. Using such approximation makes their approximate moments consistent but does not guarantee the approximate moments converge to the truth. On the other hand, we can in principle solve these moment equations by the moment quadrature as well. This gives a convergent continuous-time filter, at the cost of losing the consistency using finite number of moments. As such, our work in this paper can be seen as a convergent projection filter for discrete-time measurements.

The work in [26] (cf. [2]) similarly solves the filtering problem by moments, except that they apply Taylor expansions to solve the moment-quadrature problem and aim for the continuous-time filtering. However, as we have argued in Section 2, applying Taylor expansions to solve the moment quadrature problem imposes strict conditions on the integrands and the underlying distribution, otherwise the quadrature does not converge. During the initial phase of working on our paper, we have experimented with applying Taylor expansions, but the resulting filters numerically diverge for all the models that we show in the experiment section. Moreover, using high-order Taylor expansions is computationally hard, even with the aid of automatic differentiation. The experiments in [26] have demonstrated their method with moments of orders up to three, while ours can be up to thirty handily. It is also unclear whether the filter in [26] is in theory convergent.

The Edgeworth series are common tools to approximate probability density functions by moments, and they are used in the filtering context as well [5, 33]. The idea is to find a reference density function, and then approximate the filtering density by a product of the reference density and a polynomial of moments. If the reference density is chosen as a Gaussian, then Equations (14) and (17) can be approximated by Gauss–Hermite rules and a modification of the integrands. Essentially, this quadrature amounts to an importance integration, where the reference distribution is the importance distribution. However, in the filtering applications, it is in fact the Gram–Charlier series in [5, 33], since the Edgeworth expansion asks to decompose a random variable into independent and identically distributed ones. The convergence of the Gram–Charlier series imposes strict conditions on the tail of the distribution which limits the application of this method.

In [22], they apply the same unidimensional Gaussian quadrature as in Section 2 for approximating the distributions of SDE solutions. In a sense, solving the SDE is a special filtering problem but without the measurement variables. Hence, the work [22]

is seen as a special case of our method by discarding the update step in Algorithm 2 for unidimensional systems.

There are a number of studies that extend the Gaussian-approximate filters by leveraging high-order moments. As an example, in [19, Sec. III.C], [34], [27, Sec. V.E], and [28], they modify the unscented transform to additionally make use of the skewness and kurtosis. However, the resulting filters are still under the hood of Gaussian approximations to the true distributions. The fourth-order moment quadrature method in [11] is not restricted to the Gaussian approximation. Specifically, they represent the moments by tensors, and then use tensor decompositions of the moments to compute the quadrature rules. In principle, the quadrature method by [11] can be applied for the filtering problem as well, but it is unclear how to systematically derive the quadrature rules for moments higher than the fourth order. Even if it is possible to go beyond the fourth moment, representing the moments by tensors and computing the tensor decompositions are memory-consuming and computationally demanding.

In short, compared to the existing works, our contributions are significant in terms of the convergence and computation.

Authors' contributions. Zheng Zhao came up with the idea of the paper, did all the experiments, and wrote the initial draft. Juha Sarmavuori developed the moment quadrature methods and demonstrated them in Matlab. Juha Sarmavuori proved the convergence of the moment quadrature, and Zheng Zhao proved the convergence of the moment filter.

Acknowledgments. The authors would like to thank Adrien Corenflos for his technical suggestions on the convergence, moment matrix completion, and continuous resampling, as well as Sebastian Mair, Jens Sjölund, and Muhammad F. Emzir for their valuable comments.

REFERENCES

- [1] A. BAIN AND D. CRISAN, *Fundamentals of stochastic filtering*, vol. 60 of Stochastic Modelling and Applied Probability, Springer, 2009.
- [2] M. BOUTAYEB, M. DAROUACH, AND P. FRANK, *High order filtering for nonlinear dynamical systems*, in Proceedings of the 1997 American Control Conference, vol. 3, 1997, pp. 2177–2179.
- [3] D. BRIGO, B. HANZON, AND F. LE GLAND, *A differential geometric approach to nonlinear filtering: the projection filter*, IEEE Transactions on Automatic Control, 43 (1998), pp. 247–252.
- [4] D. BRIGO, B. HANZON, AND F. LE GLAND, *Approximate nonlinear filtering by projection on exponential manifolds of densities*, Bernoulli, 5 (1999), pp. 495–534.
- [5] S. CHALLA, Y. BAR-SHALOM, AND V. KRISHNAMURTHY, *Nonlinear filtering via generalized Edgeworth series and Gauss–Hermite quadrature*, IEEE Transactions on Signal Processing, 48 (2000), pp. 1816–1820.
- [6] S. H. CHENG AND N. J. HIGHAM, *A modified Cholesky algorithm based on a symmetric indefinite factorization*, SIAM Journal on Matrix Analysis and Applications, 19 (1998), pp. 847–1110.
- [7] N. CHOPIN AND O. PAPASPILIOPOULOS, *An introduction to sequential Monte Carlo*, Springer Series in Statistics, Springer International Publishing, 2020.
- [8] A. CORENFLOS, J. THORNTON, G. DELIGIANNIDIS, AND A. DOUCET, *Differentiable particle filtering via entropy-regularized optimal transport*, in Proceedings of the 38th International Conference on Machine Learning, vol. 139, PMLR, 2021, pp. 2100–2111.
- [9] P. DAVIS AND P. RABINOWITZ, *Methods of numerical integration*, Academic Press, 2nd ed., 1984.
- [10] C. F. DUNKL AND Y. XU, *Orthogonal polynomials of several variables*, vol. 155 of Encyclopedia of Mathematics and Its Applications, Cambridge University Press, 2nd ed., 2014.
- [11] D. C. EASLEY AND T. BERRY, *A higher order unscented transform*, SIAM/ASA Journal on Uncertainty Quantification, 9 (2021), pp. 1094–1131.

- [12] M. F. EMZIR, Z. ZHAO, AND S. SÄRKKÄ, *Multidimensional projection filters via automatic differentiation and sparse-grid integration*, Signal Processing, 204 (2023), p. 108832.
- [13] M. R. FRÉCHET AND J. A. SHOAT, *A proof of the generalized second-limit theorem in the theory of probability*, Transactions of the American Mathematical Society, 376 (1931), pp. 533–543.
- [14] W. GAUTSCHI, *Orthogonal polynomials: computation and approximation*, Numerical mathematics and scientific computation, Oxford University Press, 2004.
- [15] G. H. GOLUB AND G. MEURANT, *Matrices, moments and quadrature with applications*, Princeton series in applied mathematics, Princeton University Press, 2010.
- [16] G. H. GOLUB AND J. H. WELSCH, *Calculation of Gauss quadrature rules*, Mathematics of Computation, 23 (1969), pp. 221–230.
- [17] K. ITÔ AND K. XIONG, *Gaussian filters for nonlinear filtering problems*, IEEE Transactions on Automatic Control, 45 (2000), pp. 910–927.
- [18] A. H. JAZWINSKI, *Stochastic processes and filtering theory*, Academic Press, 1970.
- [19] S. J. JULIER, *The scaled unscented transformation*, in Proceedings of the American Control Conference, Alaska, USA, 2002, pp. 4555–4559.
- [20] R. KAN, *From moments of sum to moments of product*, Journal of Multivariate Analysis, 99 (2008), pp. 542–554.
- [21] A. KLENKE, *Probability theory: a comprehensive course*, Universitext, Springer, 2nd ed., 2014.
- [22] P. KLOEDEN AND T. SHARDLOW, *Gauss-quadrature method for one-dimensional mean-field SDEs*, SIAM Journal on Scientific Computing, 39 (2017), pp. A2395–C480.
- [23] V. I. KRYLOV, *Approximate calculation of integrals*, Dover Publications, 2005.
- [24] H. J. KUSHNER, *Approximations to optimal nonlinear filters*, IEEE Transactions on Automatic Control, 12 (1967), pp. 546–556.
- [25] K. J. H. LAW, A. M. STUART, AND K. C. ZYGALAKIS, *Data assimilation: a mathematical introduction*, Springer International Publishing Switzerland, 2015.
- [26] X. LUO, Y. JIAO, W.-L. CHIOU, AND S. S.-T. YAU, *Novel suboptimal filter via higher order central moments*, IEEE Transactions on Aerospace and Electronic Systems, 52 (2016), pp. 2030–2038.
- [27] H. M. T. MENEGAZ, J. Y. ISHIHARA, G. A. BORGES, AND A. N. VARGAS, *A systematization of the unscented Kalman filter theory*, IEEE Transactions on Automatic Control, 60 (2015), pp. 2583–2598.
- [28] K. PONOMAREVA AND P. DATE, *Higher order sigma point filter: a new heuristic for nonlinear time series filtering*, Applied Mathematics and Computation, 221 (2013), pp. 662–671.
- [29] S. SÄRKKÄ, *Bayesian filtering and smoothing*, vol. 3 of Institute of Mathematical Statistics Textbooks, Cambridge University Press, 2013.
- [30] S. SÄRKKÄ AND A. SOLIN, *Applied stochastic differential equations*, vol. 10 of Institute of Mathematical Statistics Textbooks, Cambridge University Press, 2019.
- [31] J. SARMAVUORI AND S. SÄRKKÄ, *Numerical integration as a finite matrix approximation to multiplication operator*, Journal of Computational and Applied Mathematics, 353 (2019), pp. 283–291.
- [32] B. SIMON, *Operator theory: a comprehensive course in analysis, part 4*, Institute of Mathematical Statistics Textbooks, American Mathematical Society, 2015.
- [33] H. SINGER, *Generalized Gauss–Hermite filtering*, AStA Advances in Statistical Analysis, 92 (2008), pp. 179–195.
- [34] D. TENNE AND T. SINGH, *The higher order unscented filter*, in Proceedings of the 2003 American Control Conference, vol. 3, 2003, pp. 2441–2446.
- [35] Z. ZHAO, *State-space deep Gaussian processes with applications*, PhD thesis, Aalto University, 2021.
- [36] Z. ZHAO, T. KARVONEN, R. HOSTETTLER, AND S. SÄRKKÄ, *Taylor moment expansion for continuous-discrete Gaussian filtering*, IEEE Transactions on Automatic Control, 66 (2021), pp. 4460–4467.